EUROFUSION WPJET1-CP(16) 15170

X Litaudon et al.

Overview of the JET results in support to ITER

Preprint of Paper to be submitted for publication in
Proceedings of 26th IAEA Fusion Energy Conference

This work has been carried out within the framework of the EUROfusion Consortium and has received funding from the Euratom research and training programme 2014-2018 under grant agreement No 633053. The views and opinions expressed herein do not necessarily reflect those of the European Commission.

Overview of the JET results in support to ITER

The JET contributors*

EUROfusion Consortium JET, Culham Science Centre, Abingdon, OX14 3DB, UK

e-mail contact of main author: Xavier.Litaudon@euro-fusion.org

Abstract. The 2014-2016 JET results are reviewed in the light of their significance for optimising the ITER research plan for the active and non-active operation. More than 38h of plasma operation with ITER first wall materials successfully took place. New multi-machine scaling of the type I-ELM divertor energy flux density to ITER is supported by first principle modelling. ITER relevant disruption experiments and first principle modelling are reported with a set of three disruption mitigation valves mimicking the ITER setup. Insights of the L-H power threshold in Deuterium and Hydrogen are given, stressing the importance of the magnetic configurations and the recent measurements of fine-scale structures in the edge radial electric. Dimensionless scans of the core and pedestal confinement provide new information to elucidate the importance of the first wall material on the fusion performance. H-mode plasmas at ITER triangularity (H=1 at β_N~1.8 and n/n_{GW}~0.6) have been sustained at 2MA during 5s. The ITER neutronics codes have been validated on high performance experiments. Prospects for the coming D-T campaign and 14-MeV neutron calibration strategy are reviewed.

1. Introduction

The European nuclear fusion research community has elaborated a *Roadmap to the realisation of fusion energy* in which '*ITER is the key facility and its success is the most important overarching objective of the programme*' [1]. In this overview paper, the contribution of the recent (2014-2016) JET experiments with the ITER first wall material mix [e.g. 2-8] and the underlying physics understanding with improved diagnostics are reviewed in the context of optimising the ITER research plan [10]. Indeed, together with the ITER scenario development for D-T operation [11-13], a strong focus on JET utilisation is pursued for addressing ITER needs and developing a sound physics basis for the extrapolation through first principle and integrated modelling [e.g. 14-15], e.g. plasma wall interaction, disruption mitigation for ITER taking benefit of the recent installation of a third disruption mitigation valve, L to H mode threshold scaling, core and edge confinement studies with a metallic wall, specific ITER relevant scenario aspects and preparation of the ITER non-active phase of operation (hydrogen campaign). Recent progress addressing key issues for the supporting physics research programme accompanying ITER construction is reviewed in four main sections as follows:

(i) *Plasma-material interaction studies with ITER first wall materials, in section 2*;

(ii) *Disruption prediction and mitigation studies for ITER, in section 3*;

(iii) *Access conditions to high confinement and scenario development, in section 4;*

(iv) *Nuclear fusion technology in support of ITER, in section 5*

To conclude, the prospects for the JET programme towards the integrated preparation of the coming pure tritium and deuterium-tritium experiments are discussed. Finally, the scientific benefit to further use the JET tokamak and its surrounding technology facilities beyond 2020 to train the international ITER team, up to the start of the scientific exploitation of ITER, with a possible upgrade of the heating systems and the tungsten divertor together with the ITER control tools will be briefly presented [16].

*Complete author list in the appendix

2. Plasma-material interaction studies with ITER first wall materials

The JET ITER-Like Wall (ILW) experiment provides an insight into the coupling between tokamak-plasma operation and plasma-surface interaction in the beryllium (Be) and tungsten (W) material environment and acts as a test-bed to verify physics models for ITER. In the ILW configuration with inertial cooled full W divertor and Be main chamber first wall, JET has been successfully operated with an accumulated plasma discharge time of 38 hours.

2.1 Material migration, Tritium retention and removal for ITER

Both, recent post-mortem analyses of retrieved PFCs during the last JET shutdown and gas balance studies, have confirmed a significant reduction (by factor of 10-15) of the deuterium fuel retention with the metallic first wall compared to the carbon wall [6-8, 17-24]. In addition, dust removed during the shutdown phases (2011-2012; 2013-2014) is respectively 0.8g and 1.4g, two orders of magnitude less than the JET-C wall [25-26]. The remaining retention is dominated by the retention within a Be co-deposition layer [Fig. 1 (left)] plus a smaller fraction due to implantation in the metallic wall. WallDYN simulations are able to reproduce the overall retention rate, the underlying wall material migration pattern for both the JET-C wall and JET-ILW [27], and, the gradual formation of mixed Be-W material surfaces [28]. In ITER, co-deposited layers in the divertor will be also the driving mechanism behind the tritium inventory. The ITER baseline strategy to recover the trapped tritium in the vacuum vessel is to perform baking of the PFCs, at 240°C for the Be first wall and at 350°C for the W divertor [29]. To characterise D_2 retention and release in Be co-deposited layers, a set of samples were cut from different JET-ILW regions (divertor and main chamber) for Thermal Desorption Spectrometry analyses performed at ITER-relevant bake temperatures [30-31]. Results in FIG. 1 (right) indicate that the D_2 retained fractions are varying between 40%, for the thin deposit (~3µm), up to 85% for the thickest Be deposit (40µm) even after 15h of baking at 350°C [30-31]. The experimental results were reproduced with good agreement with simulations performed with TMAP-7 calculations [29] (FIG. 1 (right)). For Be limiter samples of the main chamber, an even higher remaining retention fraction >90% is measured after baking at 240°C. The low D_2 efficiency release for thick deposits indicates that the ITER baking cycle should be further optimised or complemented by alternative schemes.

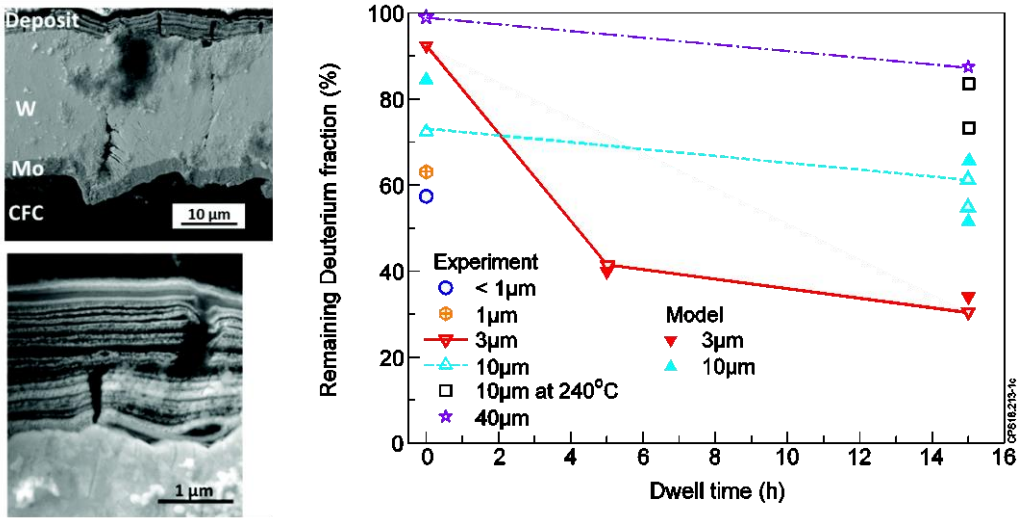

FIG. 1 (left) Layers of Be deposit on divertor tile analysed by Scanning Electron Microscopy; (right) Measured and simulated remaining D_2 fraction in Be co-deposited layers vs duration of the baking temperature duration at 350°C and 240°C (open squares); modelling with TMAP-7(filled symbols)

2.2 Type I-ELM energy flux

Multi-machine scaling of the type I-ELM divertor energy flux density parallel to magnetic field lines to ITER has been recently proposed with data from JET (CFC and ILW), ASDEX Upgrade (CFC and W walls) and MAST [32-33]. Experimental data (FIG. 2 (left)) show a linear dependence of the peak ELM energy density, $\varepsilon_{//}$ (parallel to magnetic field lines) with the pedestal top electron pressure, major radius and square root of the ELM loss energy normalised to plasma energy. This scaling provides a peak ELM energy density at the divertor target of 0.5-1.5MJ/m^2 for ITER $Q_{D\text{-}T}$=10 operation with a nominal axisymmetric divertor target surface (3° between parallel and target) and neglecting inclination and castellation of the ITER divertor. ITER predictions have been successfully compared to predictions with the non-linear MHD code JOREK [34-35]. Validation of JOREK modelling on JET was achieved by comparing the simulation results against both the JET divertor heat-flux from infra-red (IR) camera data and the ELM energy losses measured by the high-resolution Thomson scattering diagnostic. JOREK simulations reproduce the ELM energy losses for various pedestal conditions [34] (FIG. 2 (right)).

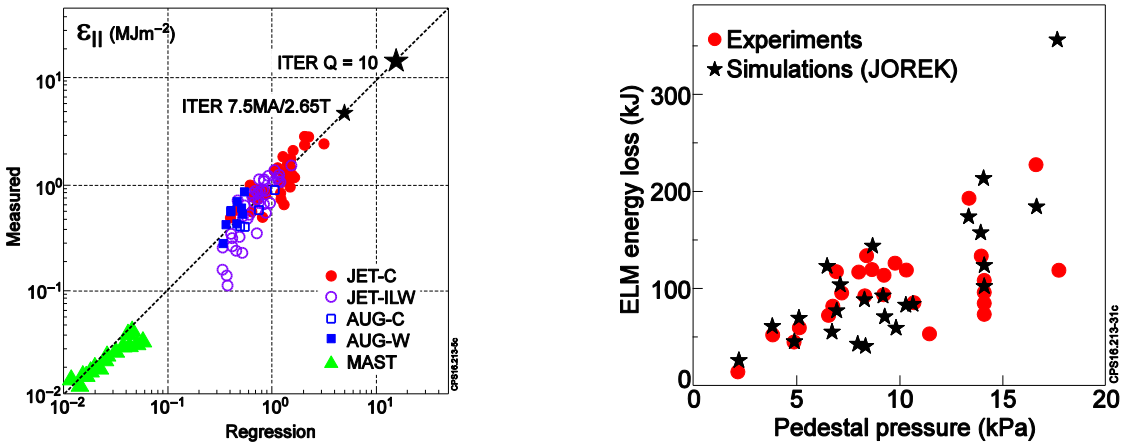

FIG. 2: (left) Scaling of type I-ELM energy flux density parallel to magnetic field lines,$\varepsilon_{//}$; (right) Simulated and measured ELM energy losses vs pedestal pressure for multiple JET-ILW pulses

2.3 Divertor heat load investigations for ITER

Another area of concern for ITER is the power handling capability of the castellated W-divertor target modules [36-37]. The underlying processes of ELM-induced transient melting, the resulting melt motion and evolution of surface morphology by re-solidified melt debris were studied following 2013 JET experiments performed using a bulk-W lamella with a protruding sloped surface structure [38-40]. One limitation of this experiment was that the IR camera did not have sufficient spatial resolution to directly resolve the melt layer temperature. The local thermal response was explained under the assumption of a significantly (60-80%) lower heat flux to the exposed leading edge than expected from geometrical projection of the parallel heat flux. A new lamella design was installed (2014-15 shutdown) where the IR camera views directly the slope exposed to the increased heat flux with improved resolution. The heat load distribution has been computed assuming the optical projection of the parallel heat flux which is determined by iteration, comparing experimental with synthetic IR data [41]. The measured heat loads, for both the old and new special geometries, no longer show discrepancy in L-mode regimes to the values from geometric projection of the parallel power flux [41] (as in COMPASS [42], ASDEX Upgrade [43]), thanks to (i) the improved special lamella geometry, and, (ii) improved modelling with the full 3-D description of the plasma heat load and heat diffusion.

3. Disruption physics for ITER

Disruption mitigation experiments carried out in different tokamaks have demonstrated the viability of Massive Gas Injection (MGI) to reduce the heat loads and electromagnetic forces. However, uncertainties in the thermal load mitigation efficiency exist due to toroidal and poloidal asymmetries of the radiation. On JET, a third Disruption Mitigation Valve (DMV) has been brought into operation since 2015, which together with the other two DMVs are at toroidal and poloidal locations mimicking the ITER set-up [44]. Dedicated JET experiments have been carried out to address ITER relevant issues [45-49]. The dynamic vertical vessel forces following MGI have been measured over a plasma current range up to I_p=3.5MA (constant configuration in either low or high triangularity) for all three injection locations separately with a similar level of injected argon (FIG. 3 (left)) [45-47]. Over the explored range of currents the unmitigated disruption force has been reduced by 33%-40% with MGI. The deduced vessel force scaling indicates that the choice of the injection location or impurity gas has practically no influence on the vessel force reduction and that the mitigation efficiency is not reduced when increasing the current. The gas amount from the mid-plane injector has been varied at 1.5MA and 2.0MA to determine the optimum impurity injection required to minimise the vertical force. A minimum of the disruption vessel force is found with a low amount of injected impurity ($\cong 1 \times 10^{22}$ particles). This is interpreted as a trade-off between the force increase induced by the eddy current with impurity injection while the force due to the halo current is reduced. ITER is aiming at radiating at least 90% of the stored thermal energy for mitigating disruptions at high plasma energy content. Initial experiments at JET carried out with one injector on top of the machine have resulted in a saturation of the radiated energy fraction (in the range of 80-85%) with increasing impurity injection [48-49]. Similar saturation levels have been observed when using the new MGI at the top location but with a higher particle throughput (factor 2) or the one located in the mid-plane. Saturation is achieved at relatively low injected impurity quantities ($\cong 1\text{-}4 \times 10^{21}$ particles). At present it cannot be concluded, due to diagnostic limitations, whether the saturation level is significantly different from unity or whether it indicates insufficient radiative energy dissipation. Thermal quench mitigation through an increase of the radiated power is feasible provided that an uneven radiated power distribution does not result in large localised radiation that will enhance the thermal loads [45]. The radiation asymmetry results from the presence of MHD activity (n=1) and from the localised injection [50]. The toroidal distribution of the radiated power is characterised by a peaking factor (ratio of maximum to average radiation). With a single injection, the toroidal peaking factor of the radiated power is up to 1.8. By optimising the MGI combining two top injectors this value has been reduced to 1.2 [45-46]. These results support the current choice of the injection locations for the ITER-disruption mitigation system.

First simulations of a D_2 MGI-triggered disruption in a purely ohmic JET plasma have been performed with the JOREK 3-D non-linear MHD code [51-52]. Simulations show that the MGI causes the consecutive growth of several magnetic island chains that leads to a formation of a stochastic layer at the plasma edge and to a fast loss of the plasma thermal energy (FIG. 3 (right)). To improve neutral gas penetration simulations, a new 1-D radial fluid code, IMAGINE, has been recently developed [53]. IMAGINE treats the neutral gas transport according to first principle convective equations and includes ionization, recombination and charge exchange atomic processes. An important result related to the question of gas penetration is the unsuccessful attempt to suppress the run-away electrons beam on JET [49], the only tokamak where run-away beam suppression using MGI is inefficient. The simulations with IMAGINE indicate that the run-away electron beam is shielded by the surrounding cold plasma (through charge exchange processes) when its

background density is large enough (10^{20} m^{-3}) to prevent neutral gas penetration. To further investigate this process, experiments have been performed by varying the background densities. In addition, it is planned to install (2016-2017 shutdown) a new Shattered Pellet Injection system (within the frame of an international collaboration) to compare with MGI and elucidate the differences between JET, DIII-D and ASDEX Upgrade experiments in view of ITER extrapolation.

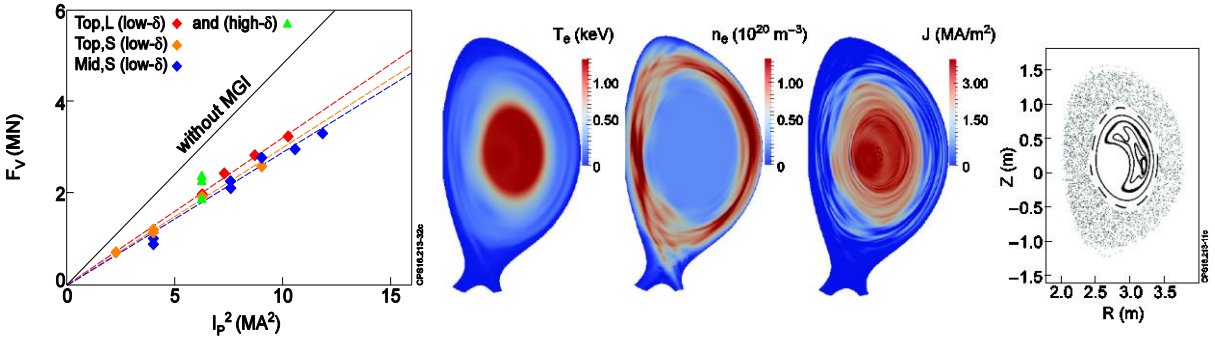

FIG. 3: (left) Vertical vessel force (F_V) vs current squared; black line: F_V for unmitigated vertical displacement events; scaling derived for each injector (dashed lines); (right) JOREK simulation of a JET disruption; poloidal cross section of electron temperature; electron density, current density and Poincare plots. JET pulse 86887 at t=5.7ms after MGI, i.e. at the start of the thermal quench

4. Access conditions to high confinement and ITER scenario development

4.1. Physics of H-mode access with ITER first wall materials

Identical deuterium discharges with the Be/W wall have shown a 25%-30% reduction of the L to H power threshold, P_{L-H}, in ASDEX Upgrade [54] and in JET [55-57] with metallic PFCs and a minimum P_{L-H} when scanning the density, that is not observed in JET-C wall. Doppler backscattering measurements have revealed novel insights into the development of the edge transport barrier thanks to high spatial resolution measurements of the edge radial electric field, E_r (FIG. 4 (right)). For the first time, fine-scale spatial structures in the E_r well, with a wave number $k_r\rho_i \approx 0.4–0.8$, consistent with stationary zonal flows (ZFs) have been observed in a tokamak [58-59]. These observations imply that stationary ZFs are crucial for the pedestal development in JET. An increase in edge $E_r \times B$ shear through the SOL radial electric field E_r is proposed as a mechanism to explain the divertor configuration effect on P_{L-H} [60]. JET experiments show a factor of two reduction of P_{LH} in a configuration with the outer strike point on the horizontal versus vertical target tiles (FIG. 4 (left)). EDGE2D-EIRENE simulations reproduce the difference in experimental target profiles, leading to a significant difference in E_r and its shear [60]. In addition, a clear correlation between detachment of the inner divertor leg to create highly asymmetric divertor conditions and the L-H transition in the high density branch is found (FIG. 5 (left)) [61]. These results indicate a strong role of the SOL in the physics of the L-H transition. Experiments have been conducted in 2014 and 2016 in hydrogen plasmas to investigate the isotope effect on P_{L-H}. It was found that P_{L-H} is increased by a factor 2 in the high density branch as was anticipated, but for the first time it has been observed that the minimum density value is shifted to higher density (ICRH only at 1.8T/1.2-1.7 MA) [61]. In addition, the dependence of P_{L-H} on isotope ratio, $n_H/(n_H+n_D)$ has been systematically investigated in 2016 by scanning the H and D mixture. It was found that P_{L-H} has a non-linear dependence with the isotope ratio. P_{L-H} is constant over a broad range of H and D mixture $20\% \leq n_H/(n_H+n_D) \leq 80\%$, with a value which is approximately an average between pure hydrogen and pure deuterium plasma. P_{L-H} sharply decreases (respectively

increases) towards the pure D (resp. H) threshold value in the two extreme parts of the curve. This result opens a new route for reducing $P_{L\text{-}H}$ in the ITER non-nuclear hydrogen phase by adding a small amount of non-reactive gas with higher atomic mass (like helium).

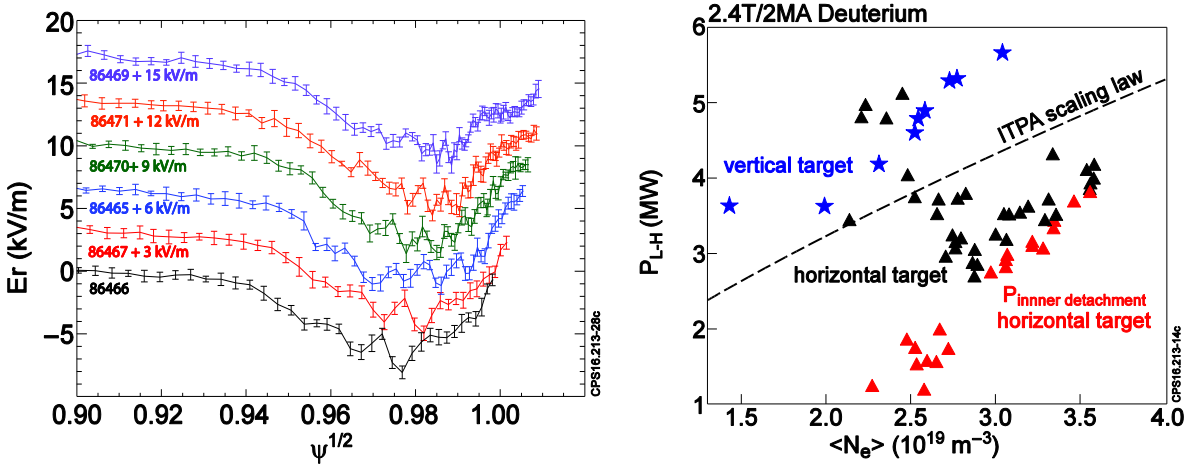

FIG. 4: (left) E_r profiles inferred from Doppler backscattering measurements in Ohmic conditions preceding the L-H transition at different densities (I_p=2.5 MA, B_t=3 T); (right) $P_{L\text{-}H}$ at 2.4T/2MA for two magnetic configurations in D_2 (vertical and horizontal target) and $P_{L\text{-}H}$ for detachment of the inner divertor leg in the horizontal target configuration (red triangles).

4.2. Core and Pedestal confinement with ITER-like wall

After the replacement of the plasma facing components, the global energy confinement for the JET-ILW was often found lower compared to JET-C, particularly when scenarios were not properly optimized [62]. These observations have an impact on the extrapolation to ITER performance. As T_e at the top of the pedestal is lower for JET-ILW, it is not obvious whether the decrease in core T_e is only due to degradation of edge confinement or if the core confinement is also degraded. A systematic interpretative heat transport analysis has been carried out where 10 pairs of 'similar' discharges for the two wall configurations have been analysed [63]. No significant change in effective heat conductivities have been found between similar pairs of discharges confirming that the core confinement is not degraded after the PFC replacement [63]. In addition dedicated heat transport experiments [64-66] have confirmed the importance of two core transport mechanisms. The first mechanism is the stabilizing effect that the gradient of the total pressure (including the fast ions) has on the ion heat transport driven by ITG instabilities [67] as confirmed by non-linear gyro-kinetic electromagnetic simulations with GENE [68] and GYRO [69]. This effect is also observed with dominant ICRH heating which is promising for ITER where low rotation but large fast ion populations are expected. The second mechanism is the capability of small radial scale ETG instabilities to carry a significant fraction of turbulent electron heat flux [65-66]. A decrease in the electron temperature gradient is correlated with the reduction Z_{eff} T_e/T_i which suggests that ETG destabilisation plays a role in the anomalous electron heat transport. Non-linear ITG/TEM turbulence simulations performed with GENE show that the ITG/TEM turbulence alone is not enough to match the experimental data. Including ETG turbulence provides a better match to the measured electron heat flux.

Three dimensionless scans in the normalized Larmor radius ρ^*, collisionality ν^* and pressure β have been performed in JET-ILW discharges [70-71]. The change from the C to the metal wall has not modified the ρ^* gyro-Bohm scaling for core and pedestal confinement (FIG. 5 (left)). The ν^* scan shows a stronger increase of the normalized energy confinement with

decreasing ν* compared to earlier JET-C results (FIG. 5 (middle)). The stronger ν* dependence with the JET-ILW is related to an improvement in the pedestal stability at low ν*. Finally, the *β* scan has revealed (FIG. 5 (right)) two different behaviours depending on ν* (not observed with the C-wall). At low ν* (ν*≅0.03), JET-ILW confinement has no clear dependence with β, in agreement with the earlier scaling. At high ν* (ν*≅0.15), a reduction of the confinement with increasing β is observed. The degradation of the JET-ILW confinement with β at high ν* is due to the reduction of the pedestal confinement since the core transport remains constant.

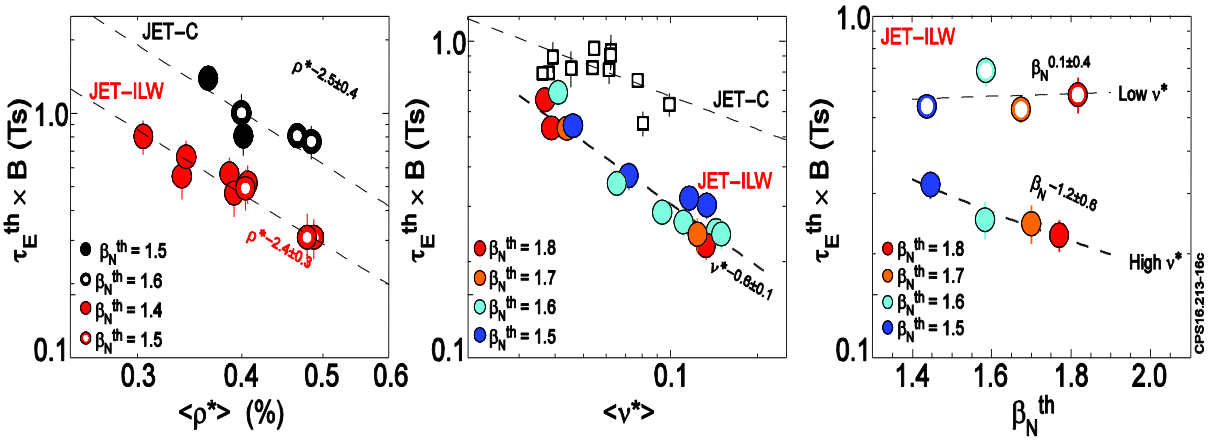

FIG. 5: Normalized thermal energy confinement versus volume averaged ρ (left), ν*(middle) and thermal β_N^{th} (right). JET-C data in black symbols. In the middle box, dashed line shows ν* trend with the JET-C as in McDonald et al., Proc. 20th Int. Conf. on Fusion Energy 2004.*

The observation that the most significant changes in the global confinement with the ILW are ascribed to the modification of the pedestal structure has motivated a significant number of studies to understand the underlying physics that affects the pedestal confinement [62, 70-79]. Recently a relative radial shift (up to 3.0% of the poloidal flux) between the electron density and the temperature pedestal position has been observed on JET [70] (as on ASDEX Upgrade [80] and DIII-D [81]) which affects the pedestal stability (FIG. 7 (left)). Comparison between JET-C and JET-ILW data baseline operational regime within the same range of β and ν* shows that JET-C discharges have systematically a smaller 'pedestal radial shift' compared to JET-ILW, and, that the normalised pedestal pressure α values decrease with the relative shift (FIG. 6 (right)) [72]. These experimental findings suggest that different plasma facing components affect the pedestal density position and pedestal stability. The edge ideal MHD stability limit calculation and comparison of the experimental results with theory are done within the framework of the peeling-ballooning (P-B) model. When assessing the edge stability, the pressure pedestals with the C-wall are consistently found close to the P-B limit. On the contrary, JET-ILW pedestal measurements show that the operational points are far from the P-B stability boundary [73]. A possible explanation is that the present MHD stability model does not consider kinetic effects such as those related to the ion diamagnetic drift and plasma rotation [78]. Furthermore, the understanding of the first wall material effect on confinement requires a coupled description of SOL, pedestal and core physics [82]. Integrated modelling suites (CRONOS [83] or JINTRAC [84]) have been coupled to pedestal models with different level of sophistication, e.g. (i) Cordey's 0-D pedestal scaling [85], or (ii) the recently developed EUROPED model [86] as an extension of EPED [87] for predictive simulation. The coupled core-pedestal simulations reproduce the observed increase in plasma stored energy with heating power and the departure from the IPB98(y,2) scaling at high power [88] thanks to a positive feedback loop between core and pedestal at high beta.

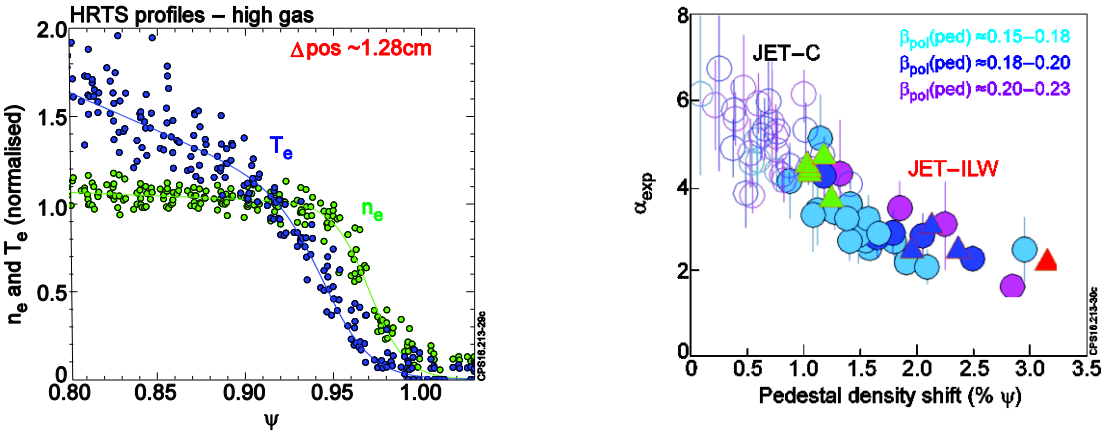

FIG. 6: (left) JET-ILW pedestal T_e and n_e profiles for high gas flow, low δ baseline pulse; (right) α vs. the 'pedestal relative shift' for JET-ILW (filled symbols) and JET-C (open symbols) low δ baseline pulses(q_{95}≈2.6 and 3, $\nu^*(ped)$ ≈ 0.1-0.35). The filled triangles correspond to a power scan at constant beta in the hybrid regime for three gas levels: low, medium, high gas injection (green, blue and red resp.) at $\nu_*(ped)$ ≈ 0.15-0.37 and $\beta_{pol}(ped)$: 0.21-0.25.

4.3. Novel three-ion ICRF heating scenarios and potential ITER application

A new ICRH absorption scheme has been proposed which hinges on the presence of three ion species [89]. Three-ion ICRH scenarios feature strong absorption of RF power at very low concentrations of minority ions by choosing a proper plasma mixture such that the L cut-off layer is located close to the third ion species cyclotron resonance. Thanks to an enhanced left-hand RF field component, RF power is efficiently absorbed even if the third ion species is present in trace quantities (~0.1%–1%). Proof of principle experiments have been carried out at JET and Alcator C-Mod [90]. Three-ion minority heating of ^{3}He ions in H-D plasma mixtures, D-(^{3}He)-H scenario, has been successfully explored on JET with ^{3}He concentrations as low as ~0.2% where 4.5 MW of ICRF power is coupled to H-D plasmas (3.2T/2MA). RF generation of energetic ^{3}He ions has been confirmed by several independent measurements. The new three-ion scenarios bring new applications and opportunities for ICRF operation, including a dedicated tool for fast-ion physics studies and new heating scenarios for JET and ITER, e.g. taking advantage that intrinsic ^{9}Be impurities are present at low levels in JET-ILW as well as on ITER with the Be first wall [91].

4.4. High-triangularity H-mode studies in JET-ILW

The achievement of high confinement at high triangularity, δ, and at high density is a necessary condition for reaching the $Q_{D\text{-}T}$=10 ITER target (H_{98}=1, β_N=1.8 and n_e/n_{Gw}=0.85) [92]. Past experiments in JET with the ILW in 2012-2014 showed that the high puff rates to keep W core radiation within acceptable limits in the baseline scenario at high-δ (δ_{av}~0.4, I_p=2.5 MA) resulted in a confinement deterioration larger (10-30%) than that observed with the C-wall [93] without showing a positive effect of δ on global confinement [62]. Only by using nitrogen seeding it was possible to partially recover the confinement at high-δ [94-95]. 2015-2016 experiments have been conducted using a new high-δ configuration (δ_{av}=0.39) with a divertor geometry optimized for pumping (both strike points in the divertor corners) [96]. In these conditions, high confinement plasmas are obtained at high-δ up to 2 MA confirming that divertor pumping is a key element to access to good confinement in ILW scenarios. These new results represent a significant improvement with respect to earlier JET-ILW results [88] and highlight the importance of operating at low ν^* to recover the beneficial effects of triangularity on pedestal stability when approaching the Peeling-Ballooning limit.

4.5 JET prospects for D-T operation

One of the main objectives of the coming D-D and D-T campaigns is to extend the performance of the ILW at higher plasma current (>2.5MA) by exploiting the JET machine capability at high additional powers around 40MW. Two approaches are being pursued at low δ configuration for the future D-T campaign [12, 97], i.e. (i) the ITER baseline scenario by increasing the current, toroidal field and applied powers at q_{95}~3 and β_N~1.8-2, (ii) the ITER hybrid scenario at reduced current and q_{95}~3-4 but at β_N>2 to enter in the virtuous cycle where confinement is increased at high beta [88]. With the available applied power in the range of 26-30MW, the JET performance has been recovered up to a plasma current of 2.5MA for both the ITER baseline and hybrid scenarios [12]. As part of the scenario development it is essential for JET and ITER that attention is given to minimize the occurrence of disruptions close to full performance, by developing disruption avoidance techniques [98]. With the goal of simultaneously increasing the fusion performance while controlling the core W content, a dual frequency ICRH heating scheme has been recently explored using both the H and ^{3}He minority heating schemes [99]. The challenge is to reach and sustain the fusion performance while not exceeding the power and energy limits imposed by the inertially cooled W-divertor. ITER relevant real time divertor detachment control algorithms have been tested on JET [100]. In addition, a strong modelling programme has been initiated with the aim of optimizing the path towards sustained D-T fusion energy [101-102]. The impact on turbulence and on fusion power of the isotope change from D-D to D-T [101] has been explored by performing simulations at maximum power and including D and T species in TGLF model [103]. With the same heating source profiles, the simulated ion and electron temperatures show a significant increase from D-D to D-T mixtures when including the isotope effect on core transport: the equivalent fusion power increases from $P_{fus}\cong$11MW to 16MW. In this context, one of the objectives of the coming pure tritium campaign will be to investigate the hydrogen isotope effects on fusion performance [104-106].

5. Nuclear technology in support of ITER

The 14MeV neutron rates from the D-T reaction should be accurately measured for the scientific exploitation of JET and ITER [107-108]. An accurate calibration procedure of 14-MeV neutron rates has been developed using a 14 MeV neutron generator (characterized in 2016 in a dedicated neutron facility) to be deployed in JET by remote handling during the 2016-2017 shutdown. In addition, dedicated neutron measurements (neutron fluence, dose-rates and activation) around JET have been performed to validate the various codes used in ITER [108]. It was demonstrated that the neutron fluence measurements are well reproduced by the Monte-Carlo codes over a range of six orders of magnitude [108]. A good agreement is found among the codes that reproduce the measured decay gamma dose rates [109] during shutdowns. This is an important step to gain confidence in ITER safety assessment calculations.

6. Conclusion and Prospects

JET and its surrounding technology facilities have a number of features that are presently unique: ITER-like wall, operation with all hydrogen isotopes, tritium and beryllium handling facilities, remote maintenance facility. We have shown that the operation of these facilities plays an important role in optimising the ITER research plan and thereby in ensuring a rapid transition to ITER D-T operation. Up to 2020[1], the focus of the JET campaigns is the

[1] pending decisions on funding EUROfusion and the JET Operating Contract in 2019-2020

preparation of the D-D, T-T and D-T campaigns and the investigation of the hydrogen isotope effects on fusion performance with the ITER material mix. Both baseline and hybrid operational regimes should progress towards ITER dimensionless parameters leading to stationary fusion performance. After the 2016-2017 shutdown, the major challenge for the 2018-2019 campaigns consists of integrating high confinement operation with the W-divertor constraints at full applied heating power. With the installation of upgraded actively cooled components, the NBI system will be capable of providing 34 MW in either deuterium or tritium [11] to further extend the performance of the ILW. In parallel, it has also been proposed to extend the life of JET beyond 2020 until the start of the scientific exploitation of ITER [16]. After a number of refurbishments and enhancements (ITER-like divertor and Electron Cyclotron Resonant Heating system, ITER-like real time control system,…) JET will be even more suited to optimise ITER operation and to train the ITER operation staff.

Acknowledgement This work has been carried out within the framework of the EUROfusion Consortium and has received funding from the Euratom research and training programme 2014-2018 under grant agreement No 633053. The views and opinions expressed herein do not necessarily reflect those of the European Commission.

References

[1] F. Romanelli et al, EFDA (2012) ISBN 978-3-00-040720-8
[2] J. Pamela et al, J. Nucl. Mater. **363–365** (2007) 1
[3] G.F. Matthews et al, Phys. Scr. **T145** (2011) 014001
[4] F. Romanelli and JET Contributors, Nucl. Fusion **55** (2015) 104001
[5] L. Horton et al, Fusion Eng. Des. **96-97** (2015) 28
[6] G.F. Matthews et al, J. Nucl. Mater. **438** (2013) S2
[7] S. Brezinsek et al, Nucl. Fusion **53** (2013) 083023
[8] G.F. Matthews et al, Phys. Scr. **T159** (2014) 014015
[9] N. Den Harder et al, Nucl. Fusion **56** (2016) 026014
[10] D.J. Campbell et al, *Challenges in Burning Plasma Physics: the ITER Research Plan*, Proc. 24th Int. Conf. on Fusion Energy (San Diego, USA 2012) ITR/P1-18
[11] L. Horton et al, Fusion Eng. and Des. **109–111** (2016) 925
[12] I. Nunes et al, Plasma Phys. Control. Fusion **58** (2016) 014034
[13] X. Litaudon et al, IEEE Transac. on Plasma Sci. (2016)
[14] G.L. Falchetto et al, this conference TH/P2-13
[15] X. Litaudon et al, Nucl. Fusion **53** (2013) 073024
[16] A.J.H. Donné, S. Cowley, T. Jones, X. Litaudon, J Fusion Energ. **35** (2016) 85
[17] R.L. Neu et al, IEEE Transact. on Plasma Sci **42** (2014) 552
[18] S. Brezinsek et al. J. Nucl. Mat, **463** (2015) 11
[19] T. Loarer et al. J. Nucl. Mat, **438** (2013) S108
[20] K. Heinola et al. J. Nucl. Mat, **463** (2015) 961
[21] A.M. Widdowson et a, Physica Scripta **T159** (2014) 014010
[22] K. Heinola, et al, Phys. Scr. **T167** (2016) 014075
[23] M. Rubel et al, this conference EX/P6-1
[24] A.M. Widdowson et al, this conference MPT/1-3
[25] E. Fortuna-Zalesna et al, this conference EX/P6-20
[26] N. Ashikawa et al, this conference EX/P6-19
[27] K. Schmid et al, Nucl. Fusion **55** (2015) 053015
[28] K. Krieger et al. J. Nucl, Mat, **438** (2013) 262
[29] G. De Temmerman et al, *Efficiency of thermal outgassing for tritium removal in ITER* Proc. 22nd Int. Conf. on Plasma Surface Int. in Cont. Fusion Devices (Rome, Italy) 2016
[30] K. Heinola et al, this conference EX/P6-2

[31] J. Likonen et al, *Deuterium trapping and release in ITER-Like co-deposited layers* Proc. 22nd Int. Conf. on Plasma Surface Int. in Cont. Fusion Devices (Rome, Italy) 2016
[32] Th. Eich et al, *ELM divertor heat load scaling to ITER with data from JET, MAST and ASDEX Upgrade* in Proc. 22nd Int. Conf. on PSI in Cont. Fusion Devices (Rome, Italy) 2016
[33] B. Sieglin et al, this conference EX/7-3Ra
[34] S. Pamela et al, Plasma Phys. Control. Fusion **58** (2016) 014026 and this conf. TH/8-2
[35] S. Futatani et al, this conference TH/P1-25
[36] S. Carpentier-Chouchana et al, Phys. Scr. **T159** (2014) 014002
[37] J.P. Gunn et al, *Ion orbit modelling of ELM heat loads on ITER divertor vertical targets* Proc. 22nd Int. Conf. on PSI. in Cont. Fusion Devices (Rome, Italy) 2016
[38] J.W. Coenen et al, Nucl. Fusion **55** (2015) 023010
[39] G. Arnoux et al. J. Nucl. Mat. **463** (2015) 415
[40] G. F. Matthews et al, Phys. Scr. **T167** (2016) 014070
[41] Y. Corre et al, this conference EX/P6-5
[42] R. Dejarnac et al, *Power loads to misaligned edges in COMPASS* Proc. 22nd Int. Conf. on Plasma Surface Int. in Cont. Fusion Devices (Rome, Italy) 2016
[43] K. Krieger et al, *Influence of inhomogeneous power flux distribution at tungsten divertor target plates on power handling capabilities* Proc. 22nd Int. Conf. on Plasma Surface Int. in Cont. Fusion Devices (Rome, Italy) 2016
[44] M. Lehnen et al, J. Nucl. Mat. **463** (2015) 39
[45] S. Jachmich et al, *Disruption mitigation experiments at JET in support of ITER* in Proc. 22nd Int. Conf. on Plasma Surface Int. in Cont. Fusion Devices (Rome, Italy) 2016
[46] S. Jachmich et al, *Disruption mitigation at JET using massive gas injection* in Proc. of 43rd European Physical Society Conf. on Plasma Physics (Leuven, Belgium) 2016
[47] E. Joffrin et al, this conference EX/9-1
[48] M. Lehnen, Nucl. Fusion **53** (2013) 093007
[49] C. Reux et al, Nucl. Fusion **55** (2015) 093013
[50] M. Lehnen et al, Nucl. Fusion **55** (2015) 123027
[51] A. Fil et al, Physics of Plasmas **22** (2015) 062509
[52] E. Nardon et al, *Progress in understanding disruptions triggered by massive gas injection via 3D non-linear MHD modelling with JOREK* Invited talk at 43rd EPS Conf. on Plasma Physics (Leuven, Belgium, 2016) to appear in Plasma Phys. Contr. Fusion
[53] E. Nardon et al, submitted Nucl Fusion (2016)
[54] F. Ryter et al, Nucl. Fusion **53** (2013) 113003
[55] C. F. Maggi et al, Nucl. Fusion **54** (2014) 023007
[56] C. Bourdelle et al, Nucl. Fusion **54** (2014) 022001
[57] E. Delabie et al, *The relation between divertor conditions and the L-H threshold on JET-ILW* Proc. of the 42nd EPS conf. on Plasma Physics (Lisbon, Portugal) 2015
[58] J. C. Hillesheim et al, Phys. Rev. Lett. **116** (2016) 065002
[59] J. C. Hillesheim et al, this conference EX/5-2
[60] A.V. Chankin et al, *Possible influence of near SOL plasma on the H-mode power threshold* Proc. 22nd Int. Conf on Plasma Surface Int. Cont. Fusion Devices (Rome, Italy) 2016
[61] E. Delabie et al, *L-H threshold experiments in hydrogen plasmas in JET-ILW* Proc. 57th Annual Meeting APS Division of Plasma Physics, Savannah, Georgia, USA (2015)
[62] M. Beurskens et al, Nucl. Fusion, **54** (2014) 043001
[63] H.T. Kim et al, Plasma Phys. Contr. Fusion **57** (2015) 065002
[64] P. Mantica et al, Phys. Rev. Lett. **107** (2011)135004
[65] P. Mantica et al, this conference EX/P6-14
[66] N. Bonanomi et al, *Impact of electron scale modes on electron heat transport in the JET tokamak* Proc. of the 42nd EPS conf. on Plasma Physics (Lisbon, Portugal) 2015

[67] J. Citrin et al, Phys. Rev. Lett. **111** (2013) 155001
[68] F. Jenko et al, Phys. Plasmas **7** (2000) 1904
[69] J. Candy and R. E.Waltz J. Comput. Phys. **186** (2003) 545
[70] L. Frassinetti et al, *Dimensionless scans in low δ baseline JET-ILW plasmas and comparison with JET-C*, Invited talk at Proc. 43rd EPS Conf. on Plasma Physics (Leuven, Belgium) 2016 to appear in Plasma Phys. Contr. Fusion
[71] L. Frassinetti et al, sub. to Nucl. Fusion (2016)
[72] E. Stefanikova et al, *Effect of the relative shift between the electron density and temperature pedestal position on the pedestal stability in JET-ILW* Proc. 43rd EPS Conf. on Plasma Physics (Leuven, Belgium) 2016
[73] C.F. Maggi et al, Nucl. Fusion **55** (2015) 113031
[74] C.F. Maggi et al, this conference EX/3-3
[75] S. Saarelma et al, Phys. Plasmas **22** (2015) 056115
[76] I.T. Chapman et al, this conference EX/3-6
[77] H. Urano et al, this conference EX/3-4
[78] N. Aiba et al, this conference TH/8-1
[79] M.J. Leyland et al, Nucl. Fusion **55** (2015) 013019
[80] M. Dunne et al, *The role of the density profile in the ASDEX Upgrade pedestal structure* Invited talk at 43rd EPS Conf. on Plasma Physics (Leuven, Belgium, 2016)
[81] T.H. Osborne et al, Nucl. Fusion **55** *(2015) 063018*
[82] J. Garcia et al, Nuc. Fusion **55** (2015) 053007
[83] F. Artaud et al, Nucl. Fusion **50** (2010) 043001
[84] M. Romanelli et al, Plasma and Fusion Research **9** (2014) 3403023
[85] J.G. Cordey et al, Nucl. Fusion **43** (2003) 670
[86] S. Saarelma et al, Private communication (2016)
[87] P.B. Snyder et al, Phys. Plasmas **16** (2009) 056118
[88] C. Challis et al, Nucl. Fusion **55** (2015) 053031
[89] Ye.O. Kazakov et al, Nucl. Fusion **55** (2015) 032001
[90] J. Wright et al, this conference EX/P3-5
[91] Ye.O. Kazakov et al, Phys. Plasmas **22** (2015) 082511
[92] A.C.C. Sips et al, this conference EX/P6-42
[93] G. Saibene et al, Plasma Phys. Control. Fusion **44** (2002) 1769
[94] C. Giroud et al, Nucl. Fusion **53** (2013) 113025
[95] C. Giroud et al, Plasma Phys. Control. Fusion **57** (2015) 035004, this conf. EX/P6-13
[96] E. De La Luna et al, this conference EX/P6-11
[97] E. Joffrin et al, Nucl. Fusion **54** (2014) 013011
[98] F.G. Rimini et al, Fusion Eng. Des. **96–97** (2015) 165
[99] D. Van Eester et al, this conference EX/P6-10
[100] C. Guillemaut et al, sub. to Plasma Phys. Contr. Fusion (2016)
[101] J. García et al, *Challenges in the extrapolation from D-D to D-T plasmas: analysis and theory based predictions* Invited talk at 43rd EPS Conf. on Plasma Physics (Leuven, Belgium, 2016) to appear in Plasma Phys. Contr. Fusion
[102] H.T. Kim et al, this conference TH/P2-17
[103] G.M. Staebler, J.E. Kinsey and R.E. Waltz, Phys. Plasmas **12** (2005) 102508
[104] R.V. Budny et al, this conference TH/P2-16
[105] S. Sharapov et al, this conference EX/P6-8
[106] H. Weisen et al, this conference EX/P6-18
[107] P. Batistoni et al, Fusion Eng. Des. **89** (2014) 896–900
[108] P. Batistoni et al, Nucl.Fusion **55** (2015) 053028
[109] R. Villari et al, Fusion Engineering and Design, **109–111** (2016) 895

Author List, the JET contributors:
S. Abduallev[35], M. Abhangi[40], P. Abreu[47], M. Afzal[6], K.M. Aggarwal[26], T. Ahlgren[90], J.H. Ahn[7], L. Aho-Mantila[100], N. Aiba[59], M. Airila[100], R. Albanese[94], V. Aldred[6], D. Alegre[82], E. Alessi[39], P. Aleynikov[49], A. Alfier[11], A. Alkseev[62], M. Allinson[6], B. Alper[6], E. Alves[47], G. Ambrosino[94], R. Ambrosino[95], L. Amicucci[79], V. Amosov[77], E. Andersson Sundén[19], M. Angelone[79], M. Anghel[74], C. Angioni[54], L. Appel[6], C. Appelbee[6], P. Arena[27], M. Ariola[95], H. Arnichand[7], S. Arshad[36], A. Ash[6], V. Aslanyan[56], O. Asunta[1], F. Auriemma[11], Y. Austin[6], L. Avotina[92], M.D. Axton[6], C. Ayres[6], M. Bacharis[21], A. Baciero[51], D. Baião[47], S. Bailey[6], A. Baker[6], I. Balboa[6], M. Balden[54], N. Balshaw[6], R. Bament[6], J.W. Banks[6], Y.F. Baranov[6], M.A. Barnard[6], D. Barnes[6], M. Barnes[24], R. Barnsley[49], A. Baron Wiechec[6], L. Barrera Orte[30], M. Baruzzo[11], V. Basiuk[7], M. Bassan[49], R. Bastow[6], A. Batista[47], P. Batistoni[79], R. Baughan[6], B. Bauvir[49], L. Baylor[63], B. Bazylev[50], J. Beal[98], P.S. Beaumont[6], M. Beckers[35], B. Beckett[6], A. Becoulet[7], N. Bekris[31], M. Beldishevski[6], K. Bell[6], F. Belli[79], M. Bellinger[6], É. Belonohy[54], N. Ben Ayed[6], N.A. Benterman[6], H. Bergsåker[37], J. Bernardo[47], M. Bernert[54], M. Berry[6], L. Bertalot[49], C. Besliu[6], M. Beurskens[55], J. Bielecki[41], T. Biewer[63], M. Bigi[11], P. Bílková[44], F. Binda[19], J.P.S. Bizarro[47], C. Björkas[90], J. Blackburn[6], K. Blackman[6], T.R. Blackman[6], P. Blanchard[29], P. Blatchford[6], V. Bobkov[54], A. Boboc[6], G. Bodnár[101], O. Bogar[17], T. Bolzonella[11], N. Bonanomi[86], F. Bonelli[50], J. Boom[54], J. Booth[6], D. Borba[31,47], D. Borodin[35], I. Borodkina[35], A. Botrugno[79], C. Bottereau[7], P. Boulting[6], C. Bourdelle[7], M. Bowden[6], C. Bower[6], C. Bowman[98], T. Boyce[6], C. Boyd[6], H.J. Boyer[6], J.M.A. Bradshaw[6], V. Braic[76], B. Breizman[96], S. Bremond[7], P.D. Brennan[6], S. Breton[7], A. Brett[6], S. Brezinsek[35], M.D.J. Bright[6], M. Brix[6], W. Broeckx[68], M. Brombin[11], A. Brosławski[57], D.P.D. Brown[6], M. Brown[6], E. Bruno[49], J. Bucalossi[7], J. Buch[40], J. Buchanan[6], M.A. Buckley[6], R. Budny[66], H. Bufferand[7], M. Bulman[6], N. Bulmer[6], P. Bunting[6], P. Buratti[79], A. Burckhart[54], A. Buscarino[27], A. Busse[6], N.K. Butler[6], I. Bykov[37], J. Byrne[6], P. Cahyna[44], G. Calabrò[79], I. Calvo[51], Y. Camenen[4], P. Camp[6], D.C. Campling[6], J. Cane[6], B. Cannas[16], A.J. Capel[6], P.J. Card[6], A. Cardinali[79], P. Carman[6], M. Carr[6], D. Carralero[54], L. Carraro[11], B.B. Carvalho[47], I. Carvalho[47], P. Carvalho[47], F.J. Casson[6], C. Castaldo[79], N. Catarino[47], J. Caumont[6], F. Causa[79], R. Cavazzana[11], K. Cave-Ayland[6], M. Cavinato[11], M. Cecconello[19], S. Ceccuzzi[79], E. Cecil[66], A. Cenedese[11], R. Cesario[79], C.D. Challis[6], M. Chandler[6], D. Chandra[40], C.S. Chang[66], A. Chankin[54], I.T. Chapman[6], S.C. Chapman[25], M. Chernyshova[43], G. Chitarin[11], G. Ciraolo[7], D. Ciric[6], J. Citrin[34], F. Clairet[7], E. Clark[6], M. Clark[6], R. Clarkson[6], D. Clatworthy[6], C. Clements[6], M. Cleverly[6], J.P. Coad[6], P.A. Coates[6], A. Cobalt[6], V. Coccorese[94], V. Cocilovo[79], S. Coda[29], R. Coelho[47], J.W. Coenen[35], I. Coffey[26], L. Colas[7], S. Collins[6], S. Conroy[19], N. Conway[6], D. Coombs[6], D. Cooper[6], S.R. Cooper[6], C. Corradino[27], Y. Corre[7], G. Corrigan[6], S. Cortes[47], D. Coster[54], A.S. Couchman[6], M.P. Cox[6], T. Craciunescu[75], S. Cramp[6], R. Craven[6], F. Crisanti[79], G. Croci[86], D. Croft[6], K. Crombé[14], R. Crowe[6], N. Cruz[47], G. Cseh[101], A. Cullen[6], M. Curuia[74], A. Czarnecka[43], H. Dabirikhah[6], P. Dalgliesh[6], S. Dalley[6], J. Dankowski[41], D. Darrow[66], O. Davies[6], W. Davis[49,66], C. Day[50], I.E. Day[6], M. De Bock[49], A. de Castro[51], E. de la Cal[51], E. de la Luna[51], G. De Masi[11], J. L. de Pablos[51], G. De Tommasi[94], P. de Vries[49], K. Deakin[6], J. Deane[6], F. Degli Agostini[11], R. Dejarnac[44], E. Delabie[34], N. den Harder[34], R.O. Dendy[6], J. Denis[7], P. Denner[35], S. Devaux[54,93], P. Devynck[7], F. Di Maio[49], C. Di Troia[79], P. Dinca[75], T. Dittmar[35], R.P. Doerner[8], T. Donné[30], S.E. Dorling[6], S. Dormido-Canto[82], S. Doswon[6], D. Douai[7], P.T. Doyle[6], A. Drenik[54,71], P. Drewelow[55], P. Drews[35], Ph. Duckworth[49], R. Dumont[7], P. Dumortier[52], D. Dunai[101], M. Dunne[54], I. Ďuran[44], F. Durodié[52], P. Dutta[40], B. P. Duval[29], R. Dux[54], K. Dylst[68], N. Dzysiuk[19], P.V. Edappala[40], J. Edmond[6], A.M. Edwards[6], J. Edwards[6], Th. Eich[54], A. Ekedahl[7], R. El-Jorf[6], C.G. Elsmore[6], M. Enachescu[73], G. Ericsson[19], F. Eriksson[15], J. Eriksson[19], L.G. Eriksson[32], B. Esposito[79], H.G. Esser[35], D. Esteve[7], B. Evans[6], G.E. Evans[6], G. Evison[6], G.D. Ewart[6], D. Fagan[6], M. Faitsch[54], D. Falie[75], A. Fanni[16], A. Fasoli[29], J. M. Faustin[29], N. Fawlk[6], L. Fazendeiro[47], N.

Fedorczak[7], R.C. Felton[6], K. Fenton[6], A. Fernades[47], H. Fernandes[47], J. Ferreira[47], J.A. Fessey[6], O. Février[7], A. Field[6], S. Fietz[54], A. Figueiredo[47], J. Figueiredo[47,31], A. Fil[7], P. Finburg[6], M. Firdaouss[7], U. Fischer[50], L. Fittill[6], M. Fitzgerald[6], D. Flammini[79], J. Flanagan[6], C. Fleming[6], K. Flinders[6], J. M. Fontdecaba[51], A. Formisano[69], L. Forsythe[6], L. Fortuna[27], M. Fortune[6], S. Foster[6], T. Franklin[6], M. Frasca[27], L. Frassinetti[37], M. Freisinger[35], R. Fresa[87], D. Frigione[79], V. Fuchs[44], D. Fuller[31], S. Futatani[5], J. Fyvie[6], K. Gál[30,54], D. Galassi[2], K. Gałązka[43], J. Galdon-Quiroga[81], J. Gallagher[6], D. Gallart[5], R. Galvão[9], X. Gao[45], Y. Gao[35], J. Garcia[7], A. Garcia-Carrasco[37], M. García-Muñoz[81], J.-L. Gardarein[3], L. Garzotti[6], P. Gaudio[84], E. Gauthier[7], D.F. Gear[6], S.J. Gee[6], B. Geiger[54], M. Gelfusa[84], S. Gerasimov[6], G. Gervasini[39], M. Gethins[6], Z. Ghani[6], M. Ghate[40], M. Gherendi[75], J.C. Giacalone[7], L. Giacomelli[39], C.S. Gibson[6], T. Giegerich[50], C. Gil[7], L. Gil[47], S. Gilligan[6], D. Gin[48], E. Giovannozzi[79], J.B. Girardo[7], C. Giroud[6], G. Giruzzi[7], S. Glöggler[54], J. Godwin[6], J. Goff[6], P. Gohil[38], V. Goloborod'ko[91], R. Gomes[47], B. Gonçalves[47], M. Goniche[7], M. Goodliffe[6], A. Goodyear[6], G. Gorini[86], M. Gosk[57], R. Goulding[66], A. Goussarov[68], R. Gowland[6], B. Graham[6], M.E. Graham[6], J. P. Graves[29], N. Grazier[6], P. Grazier[6], N.R. Green[6], H. Greuner[54], F.S. Griph[6], C. Grisolia[7], D. Grist[6], M. Groth[1], R. Grove[63], C.N. Grundy[6], D. Guard[6], C. Guérard[30], C. Guillemaut[7,47], R. Guirlet[7], C. Gurl[6], H. H Utoh[59], L.J. Hackett[6], S. Hacquin[7,31], A. Hagar[6], A. Hakola[100], M. Halitovs[92], S.J. Hall[6], S.P. Hallworth Cook[6], C. Hamlyn-Harris[6], K. Hammond[6], C. Harrington[6], J. Harrison[6], D. Harting[6], F. Hasenbeck[35], T.D.V. Haupt[6], J. Hawes[6], N.C. Hawkes[6], J. Hawkins[6], P. Hawkins[6], P.W. Haydon[6], N. Hayter[6], S. Hazel[6], P.J.L. Heesterman[6], K. Heinola[90], C. Hellesen[19], T. Hellsten[37], W. Helou[7], O.N. Hemming[6], T.C. Hender[6], M. Henderson[49], S.S. Henderson[18], R. Henriques[47], D. Hepple[6], G. Hermon[6], P. Hertout[7], C. Hidalgo[51], E.G. Highcock[24], M. Hill[6], J. Hillairet[7], J. Hillesheim[6], D. Hillis[63], K. Hizanidis[60], A. Hjalmarsson[19], J. Hobirk[54], E. Hodille[7], C.H.A. Hogben[6], G.M.D. Hogeweij[34], A. Hollingsworth[6], S. Hollis[6], D.A. Homfray[6], J. Horáček[44], G. Hornung[14], A.R. Horton[6], L.D. Horton[32], L. Horvath[98], S.P. Hotchin[6], M.R. Hough[6], P.J. Howarth[6], A. Hubbard[56], A. Huber[35], V. Huber[35], T.M. Huddleston[6], M. Hughes[6], C.L. Hunter[6], P. Huynh[7], A.M. Hynes[6], D. Iglesias[6], N. Imazawa[59], M. Imríšek[44], M. Incelli[97], P. Innocente[11], I. Ivanova-Stanik[43], S. Jachmich[52,31], P. Jacquet[6], J. Jansons[92], A. Jardin[7], A. Järvinen[1], F. Jaulmes[34], S. Jednoróg[43], I. Jenkins[6], I. Jepu[75], E. Joffrin[7], R. Johnson[6], T. Johnson[37], Jane Johnston[6], L. Joita[6], G. Jones[6], T.T.C. Jones[6], K. K Hoshino[59], A. Kallenbach[54], K. Kamiya[59], J. Kaniewski[6], A. Kantor[6], A. Kappatou[54], J. Karhunen[1], D. Karkinsky[6], I. Karnowska[6], M. Kaufman[63], G. Kaveney[6], Y. Kazakov[52], V. Kazantzidis[60], D.L. Keeling[6], T. Keenan[6], J. Keep[6], M. Kempenaars[6], C. Kennedy[6], D. Kenny[6], J. Kent[6], O.N. Kent[6], E. Khilkevich[48], H.T. Kim[31], H.S. Kim[70], A. Kinch[6], C. king[6], D. King[6], R.F. King[6], D.J. Kinna[6], V. Kiptily[6], A. Kirk[6], K. Kirov[6], A. Kirschner[35], G. Kizane[92], C. Klepper[63], A. Klix[50], P. Knight[6], S.J. Knipe[6], S. Knott[85], T. Kobuchi[59], F. Köchl[99], G. Kocsis[101], I. Kodeli[71], L. Kogan[6], D. Kogut[7], S. Koivuranta[100], Y. Kominis[60], M. Köppen[35], T. Koskela[1], H.R. Koslowski[35], M. Koubiti[4], M. Kovari[6], E. Kowalska-Strzęciwilk[43], A. Krasilnikov[77], V. Krasilnikov[77], N. Krawczyk[43], K. Krieger[54], A. Krivska[52], U. Kruezi[6], I. Książek[42], A. Kukushkin[62], A. Kundu[40], T. Kurki-Suonio[1], O.J. Kwon[12], L. Laguardia[39], A. Laing[6], N. Lam[6], H.T. Lambertz[35], C. Lane[6], P.T. Lang[54], S. Lanthaler[29], J. Lapins[92], A. Lasa[90], J.R. Last[6], E. Łaszyńska[43], R. Lawless[6], A. Lawson[6], K.D. Lawson[6], A. Lazaros[60], E. Lazzaro[39], S. Lee[58], X. Lefebvre[6], H.J. Leggate[28], J. Lehmann[6], M. Lehnen[49], D. Leichtle[36], P. Leichuer[6], F. Leipold[49,72], I. Lengar[71], M. Lennholm[32], E. Lerche[52], A. Lescinskis[92], S. Lesnoj[6], E. Letellier[6], M. Leyland[98], W. Leysen[68], L. Li[35], Y. Liang[35], J. Likonen[100], J. Linke[35], Ch. Linsmeier[35], B. Lipschultz[98], X. Litaudon[7,31], G. Liu[49], Y. Liu[45], V.P. Lo Schiavo[94], T. Loarer[7], A. Loarte[49], R.C. Lobel[6], B. Lomanowski[1], P.J. Lomas[6], J. Lönnroth[1,31], J. M. López[83], J. López-Razola[51], R. Lorenzini[11], U. Losada[51], A.B. Loving[6], C. Lowry[32], T. Luce[38], R.M.A. Lucock[6], A. Lukin[64], M. Lungaroni[84], C.P. Lungu[75], M. Lungu[75], I. Lupelli[6], A. Lyssoivan[52], N. Macdonald[6], P. Macheta[6], K. Maczewa[6], B. Magesh[40], P.

Maget[7], C. Maggi[6], H. Maier[54], J. Mailloux[6], T. Makkonen[1], R. Makwana[40], A. Malaquias[47], A. Malizia[84], A. Manning[6], M.E. Manso[47], P. Mantica[39], M. Mantsinen[5], A. Manzanares[80], Ph. Maquet[49], Y. Marandet[4], N. Marcenko[77], C. Marchetto[39], O. Marchuk[35], M. Marinelli[84], M. Marinucci[79], T. Markovič[44], D. Marocco[79], L. Marot[23], C.A. Marren[6], R. Marshal[6], A. Martin[6], Y. Martin[29], A. Martín de Aguilera[51], J. R. Martín-Solís[13], Y. Martynova[35], S. Maruyama[49], A. Masiello[11], M. Maslov[6], S. Matejcik[17], M. Mattei[69], G.F. Matthews[6], F. Maviglia[10], M. Mayer[54], M.L. Mayoral[30], T. May-Smith[6], D. Mazon[7], C. Mazzotta[79], R. McAdams[6], P.J. McCarthy[85], K.G. McClements[6], O. McCormack[11], P.A. McCullen[6], D. McDonald[30], S. McIntosh[6], R. McKean[6], J. McKehon[6], R.C. Meadows[6], A. Meakins[6], F. Medina[51], M. Medland[6], S. Medley[6], S. Meigh[6], A.G. Meigs[6], G. Meisl[54], S. Meitner[63], L. Meneses[47], S. Menmuir[6,37], I.R. Merrigan[6], Ph. Mertens[35], S. Meshchaninov[77], A. Messiaen[52], H. Meyer[6], S. Mianowski[57], R. Michling[49], D. Middleton-Gear[6], J. Miettunen[1], F. Militello[6], E. Militello-Asp[6], G. Miloshevsky[67], F. Mink[54], S. Minucci[94], Y. Miyoshi[59], J. Mlynář[44], D. Molina[7], I. Monakhov[6], M. Moneti[97], R. Mooney[6], S. Moradi[33], S. Mordijck[38], L. Moreira[6], R. Moreno[51], F. Moro[79], A.W. Morris[6], J. Morris[6], L. Moser[23], S. Mosher[63], D. Moulton[6,1], A. Murari[11,31], A. Muraro[39], S. Murphy[6], N. N Asakura[59], F. Nabais[47], R. Naish[6], T. Nakano[59], E. Nardon[7], V. Naulin[72], M.F.F. Nave[47], I. Nedzelski[47], G. Nemtsev[77], F. Nespoli[29], A. Neto[36], R. Neu[54], M. Newman[6], K.J. Nicholls[6], A.H. Nielsen[72], P. Nielsen[11], E. Nilsson[7], D. Nishijima[88], C. Noble[6], M. Nocente[86], D. Nodwell[6], K. Nordlund[90], H. Nordman[15], R. Nouailletas[7], I. Nunes[47], M. Oberkofler[54], T. Odupitan[6], M.T. Ogawa[59], T. O'Gorman[6], M. Okabayashi[66], R. Olney[6], O. Omolayo[6], M. O'Mullane[18], J. Ongena[52], F. Orsitto[10], J. Orszagh[17], B.I. Oswuigwe[6], R. Otin[6], A. Owen[6], R. Paccagnella[11], N. Pace[6], D. Pacella[79], A. Page[6], E. Pajuste[92], S. Palazzo[27], S. Pamela[6], S. Panja[40], P. Papp[17], V. Parail[6], M. Park[58], F. Parra Diaz[24], M. Parsons[63], R. Pasqualotto[11], A. Patel[6], S. Pathak[40], D. Paton[6], H. Patten[29], A. Pau[16], E. Pawelec[42], A. Peackoc[32], I.J. Pearson[6], S.-P. Pehkonen[100], E. Peluso[84], C. Penot[49], A. Pereira[51], R. Pereira[47], C. Perez von Thun[31,35], S. Peruzzo[11], S. Peschanyi[50], M. Peterka[44], P. Petersson[37], G. Petravich[101], A. Petre[73], N. Petrella[6], V. Petržilka[44], Y. Peysson[7], D. Pfefferlé[29], V. Philipps[35], M. Pillon[79], G. Pintsuk[35], P. Piovesan[11], A. Pires dos Reis[46], A. Pironti[94], F. Pisano[16], R. Pitts[49], V. Plyusnin[47], N. Pomaro[11], O.G. Pompilian[75], P.J. Pool[6], S. Popovichev[6], M.T. Porfiri[79], C. Porosnicu[75], M. Porton[6], G. Possnert[19], S. Potzel[54], T. Powell[6], J. Pozzi[6], V. Prajapati[40], R. Prakash[40], G. Prestopino[84], D. Price[6], M. Price[6], R. Price[6], P. Prior[6], R. Proudfoot[6], G. Pucella[79], P. Puglia[46], M.E. Puiatti[11], D. Pulley[6], K. Purahoo[6], Th. Pütterich[54], E. Rachlew[22], M. Rack[35], R. Ragona[52], M.S.J. Rainford[6], A. Rakha[5], G. Ramogida[79], S. Ranjan[40], J.J. Rasmussen[72], K. Rathod[40], G. Rattá[51], G. Ravera[79], C. Rayner[6], M. Rebai[86], D. Reece[6], A. Reed[6], D. Réfy[101], B. Regan[6], J. Regaña[30], M. Reich[54], N. Reid[6], F. Reimold[35], M. Reinhart[30], M. Reinke[63], D. Reiser[35], D. Rendell[6], C. Reux[7], S. Reynolds[6], V. Riccardo[6], N. Richardson[6], K. Riddle[6], D. Rigamonti[86], F.G. Rimini[6], J. Risner[63], M. Riva[79], C. Roach[6], R.J. Robins[6], S.A. Robinson[6], T. Robinson[6], D.W. Robson[6], R. Rodionov[77], P. Rodrigues[47], J. Rodriguez[6], V. Rohde[54], F. Romanelli[79], M. Romanelli[6], S. Romanelli[6], J. Romazanov[35], S. Rowe[6], M. Rubel[37], G. Rubinacci[94], G. Rubino[11], L. Ruchko[46], M. Ruiz[83], C. Ruset[75], J. Rzadkiewicz[57], S. Saarelma[6], R. Sabot[7], E. Safi[90], P. Sagar[6], G. Saibene[36], F. Saint-Laurent[7], M. Salewski[72], A. Salmi[100], R. Salmon[6], F. Salzedas[47], D. Samaddar[6], U. Samm[35], D. Sandiford[6], P. Santa[40], M.I.K. Santala[1], B. Santos[47], A. Santucci[79], F. Sartori[36], R. Sartori[36], O. Sauter[29], R. Scannell[6], T. Schlummer[35], V. Schmidt[11], S. Schmuck[6], M. Schneider[7], K. Schöpf[91], D. Schwörer[28], S.D. Scott[66], G. Sergienko[35], M. Sertoli[54], A. Shabbir[14], S.E. Sharapov[6], A. Shaw[6], R. Shaw[6], H. Sheikh[6], A. Shepherd[6], A. Shevelev[48], A. Shumack[34], G. Sias[16], M. Sibbald[6], B. Sieglin[54], S. Silburn[6], A. Silva[47], C. Silva[47], P.A. Simmons[6], J. Simpson[6], J. Simpson-Hutchinson[6], A. Sinha[40], S.K. Sipilä[1], A.C.C. Sips[32], P. Sirén[100], A. Sirinelli[49], H. Sjöstrand[19], M. Skiba[19], R. Skilton[6], B. Slade[6], N. Smith[6], P.G. Smith[6], R. Smith[6], T.J. Smith[6], M. Smithies[98], L. Snoj[71], S. Soare[74], E.

R. Solano[31,51], A. Somers[28], C. Sommariva[7], P. Sonato[11], A. Sopplesa[11], J. Sousa[47], C. Sozzi[39], S. Spagnolo[11], T. Spelzini[6], F. Spineanu[75], G. Stables[6], I. Stamatelatos[61], M.F. Stamp[6], P. Staniec[6], G. Stankūnas[53], C. Stan-Sion[73], M.J. Stead[6], E. Stefanikova[37], I. Stepanov[52], A.V. Stephen[6], M. Stephen[40], A. Stevens[6], B.D. Stevens[6], J. Strachan[66], P. Strand[15], P. Ström[37], G. Stubbs[6], W. Studholme[6], F. Subba[65], H.P. Summers[18], J. Svensson[55], Ł. Świderski[57], T. Szabolics[101], M. Szawlowski[43], G. Szepesi[6], T. T Suzuki[59], B. Tál[101], T. Tala[100], A.R. Talbot[6], C. Taliercio[11], P. Tamain[7], C. Tame[6], M. Tardocchi[39], L. Taroni[11], D. Taylor[6], K.A. Taylor[6], D. Tegnered[15], G. Telesca[14], N. Teplova[48], D. Terranova[11], D. Testa[29], E. Tholerus[37], J. Thomas[6], J.D. Thomas[6], P. Thomas[49], A. Thompson[6], C.-A. Thompson[6], V.K. Thompson[6], L. Thorne[6], A. Thornton[6], A.S. Thrysøe[72], P.A. Tigwell[6], N. Tipton[6], I. Tiseanu[75], H. Tojo[59], M. Tomeš[44], P. Tonner[6], M. Towndrow[6], P. Trimble[6], M. Tripsky[52], M. Tsalas[34], D. Tskhakaya jun[91], I. Turner[6], M.M. Turner[28], M. Turnyanskiy[30], G. Tvalashvili[6], S.G.J. Tyrrell[6], A. Uccello[39], Z. Ul-Abidin[6], J. Uljanovs[1], D. Ulyatt[6], H. Urano[59], I. Uytdenhouwen[68], A.P. Vadgama[6], D. Valcarcel[6], M. Valentinuzzi[7], M. Valisa[11], P. Vallejos Olivares[37], M. Valovic[6], M. Van De Mortel[6], D. Van Eester[52], W. Van Renterghem[68], G.J. van Rooij[34], J. Varje[1], S. Varoutis[50], S. Vartanian[7], K. Vasava[40], J. Vega[51], G. Verdoolaege[52], R. Verhoeven[6], C. Verona[84], G. Verona Rinati[84], E. Veshchev[49], J. Vicente[47], E. Viezzer[54,81], S. Villari[79], F. Villone[89], P. Vincenzi[11], I. Vinyar[64], B. Viola[79], A. Vitins[92], Z. Vizvary[6], M. Vlad[75], I. Voitsekhovitch[30], P. Vondráček[44], N. Vora[6], T. Vu[7], W. W Pires de Sa[46], B. Wakeling[6], C.W.F. Waldon[6], N. Walkden[6], M. Walker[6], R. Walker[6], M. Walsh[49], E. Wang[35], N. Wang[35], S. Warder[6], R.J. Warren[6], J. Waterhouse[6], N.W. Watkins[25], C. Watts[49], T. Wauters[52], A. Weckmann[37], J. Weiland[20], H. Weisen[29], M. Weiszflog[19], C. Wellstood[6], A.T. West[6], M.R. Wheatley[6], S. Whetham[6], A.M. Whitehead[6], B.D. Whitehead[6], A.M. Widdowson[6], S. Wiesen[35], J. Wilkinson[6], J. Williams[6], M. Williams[6], A.R. Wilson[6], D.J. Wilson[6], H.R. Wilson[98], J. Wilson[6], M. Wischmeier[54], G. Withenshaw[6], A. Withycombe[6], D.M. Witts[6], D. Wood[6], R. Wood[6], C. Woodley[6], S. Wray[6], J. Wright[6], J. Wu[78], A. Wynn[98], T. Xu[6], D. Yadikin[15], W. Yanling[35], L. Yao[78], V. Yavorskij[91], M.G. Yoo[70], C. Young[6], D. Young[6], I.D. Young[6], R. Young[6], J. Zacks[6], R. Zagorski[43], F.S. Zaitsev[17], R. Zanino[65], A. Zarins[92], K.D. Zastrow[6], M. Zerbini[79], Y. Zhou[37], E. Zilli[11], V. Zoita[75], S. Zoletnik[101], I. Zychor[57],

[1]Aalto University, P.O.Box 14100, FIN-00076 Aalto, Finland,

[2]Aix Marseille Université, CNRS, Centrale Marseille, M2P2 UMR 7340, 13451, Marseille, France,

[3]Aix-Marseille Université, CNRS, IUSTI UMR 7343, 13013 Marseille, France,

[4]Aix-Marseille Université, CNRS, PIIM, UMR 7345, 13013 Marseille, France,

[5]Barcelona Supercomputing Center, Barcelona, Spain,

[6]CCFE, Culham Science Centre, Abingdon, Oxon, OX14 3DB, UK,

[7]CEA, IRFM, F-13108 Saint Paul Lez Durance, France,

[8]Center for Energy Research, University of California at San Diego, La Jolla, CA 92093, USA,

[9]Centro Brasileiro de Pesquisas Fisicas, Rua Xavier Sigaud, 160, Rio de Janeiro CEP 22290-180, Brazil,

[10]Consorzio CREATE, Via Claudio 21, 80125 Napoli, Italy,

[11]Consorzio RFX, corso Stati Uniti 4, 35127 Padova, Italy,

[12]Daegu University, Jillyang, Gyeongsan, Gyeongbuk 712-174, Republic of Korea,

[13]Departamento de Física, Universidad Carlos III de Madrid, 28911 Leganés, Madrid, Spain,

[14]Department of Applied Physics UG (Ghent University) St-Pietersnieuwstraat 41 B-9000 Ghent, Belgium,

[15]Department of Earth and Space Sciences, Chalmers University of Technology, SE-41296 Gothenburg, Sweden,

[16]Department of Electrical and Electronic Engineering, University of Cagliari, Piazza d'Armi 09123 Cagliari, Italy,
[17]Department of Experimental Physics, Faculty of Mathematics, Physics and Informatics Comenius University Mlynska dolina F2, 84248 Bratislava, Slovak Republic,
[18]Department of Physics and Applied Physics, University of Strathclyde, Glasgow, G4 ONG, UK,
[19]Department of Physics and Astronomy, Uppsala University, SE-75120 Uppsala, Sweden,
[20]Department of Physics, Chalmers University of Technology, SE-41296 Gothenburg, Sweden,
[21]Department of Physics, Imperial College London, SW7 2AZ, UK,
[22]Department of Physics, SCI, KTH, SE-10691 Stockholm, Sweden,
[23]Department of Physics, University of Basel, Switzerland ,
[24]Department of Physics, University of Oxford, OX1 2JD, UK,
[25]Department of Physics, University of Warwick, Coventry, CV4 7AL, UK,
[26]Department of Pure and Applied Physics, Queens University, Belfast, BT7 1NN, UK,
[27]Dipartimento di Ingegneria Elettrica Elettronica e Informatica-Università degli Studi di Catania, 95125 Catania, Italy,
[28]Dublin City University (DCU), Ireland,
[29]Ecole Polytechnique Fédérale de Lausanne (EPFL), Swiss Plasma Center (SPC), CH-1015 Lausanne, Switzerland,
[30]EUROfusion Programme Management Unit, Boltzmannstr. 2, 85748 Garching, Germany,
[31]EUROfusion Programme Management Unit, Culham Science Centre, Culham, OX14 3DB, UK ,
[32]European Commission, B-1049 Brussels, Belgium,
[33]Fluid and Plasma Dynamics, ULB - Campus Plaine - CP 231 Boulevard du Triomphe, 1050 Bruxelles, Belgium,
[34]FOM Institute DIFFER, Eindhoven, the Netherlands,
[35]Forschungszentrum Jülich GmbH, Institut für Energie- und Klimaforschung - Plasmaphysik, 52425 Jülich, Germany,
[36]Fusion for Energy Joint Undertaking, Josep Pl. 2, Torres Diagonal Litoral B3, 08019, Barcelona, Spain,
[37]Fusion Plasma Physics, EES, KTH, SE-10044 Stockholm, Sweden,
[38]General Atomics, P.O.Box 85608, San Diego, CA 92186-5608, California, USA,
[39]IFP-CNR, via R. Cozzi 53, 20125 Milano, Italy,
[40]Institute for Plasma Research, Bhat, Gandhinagar - 382 428, Gujarat State, India,
[41]Institute of Nuclear Physics, Radzikowskiego 152, 31-342 Kraków, Poland,
[42]Institute of Physics, Opole University, Oleska 48, 45-052 Opole, Poland,
[43]Institute of Plasma Physics and Laser Microfusion, Hery 23, 01-497 Warsaw, Poland,
[44]Institute of Plasma Physics AS CR, Za Slovankou 1782/3, 182 00 Praha 8, Czech Republic,
[45]Institute of Plasma Physics, Chinese Academy of Sciences, Hefei, 230031, China,
[46]Instituto de Física - Universidade de São Paulo Rua do Matão Travessa R Nr.187 CEP 05508-090 Cidade Universitária, São Paulo, Brasil ,
[47]Instituto de Plasmas e Fusão Nuclear, Instituto Superior Técnico, Universidade de Lisboa, Portugal,
[48]Ioffe Physico-Technical Institute, 26 Politekhnicheskaya, St Petersburg 194021, Russian Federation,
[49]ITER Organization, Route de Vinon, CS 90 046, 13067 Saint Paul Lez Durance, France,
[50]Karlsruhe Institute of Technology, P.O.Box 3640, D-76021 Karlsruhe, Germany,
[51]Laboratorio Nacional de Fusión, CIEMAT, Madrid, Spain,

[52]Laboratory for Plasma Physics Koninklijke Militaire School - Ecole Royale Militaire Renaissancelaan 30 Avenue de la Renaissance B-1000, Brussels, Belgium,
[53]Lithuanian energy institute, Breslaujos g. 3, LT-44403, Kaunas, Lithuania,
[54]Max-Planck-Institut für Plasmaphysik, D-85748 Garching, Germany,
[55]Max-Planck-Institut für Plasmaphysik, Teilinsitut Greifswald, D-17491 Greifswald, Germany,
[56]MIT Plasma Science and Fusion Centre, Cambridge, MA 02139, Massachusetts, USA,
[57]National Centre for Nuclear Research(NCBJ),05-400 Otwock-Świerk, Poland,
[58]National Fusion Research Institute(NFRI) 169-148 Gwahak-ro, Yuseong-gu, Daejeon 305-806, Republic of Korea,
[59]National Institutes for Quantum and Radiological Science and Technology, Naka, Ibaraki 311-0193, Japan,
[60]National Technical University of Athens, Iroon Politechniou 9, 157 73 Zografou, Athens, Greece,
[61]NCSR "Demokritos" 153 10, Agia Paraskevi Attikis, Greece,
[62]NRC Kurchatov Institute, 1 Kurchatov Square, Moscow 123182, Russian Federation,
[63]Oak Ridge National Laboratory, Oak Ridge, TN 37831-6169, Tennessee, USA,
[64]PELIN LLC, 27a, Gzhatskaya Ulitsa, Saint Petersburg, 195220, Russian Federation,
[65]Politecnico di Torino, Corso Duca degli Abruzzi 24, I-10129 Torino, Italy,
[66]Princeton Plasma Physics Laboratory, James Forrestal Campus, Princeton, NJ 08543, New Jersey, USA,
[67]Purdue University, 610 Purdue Mall, West Lafayette, IN 47907, USA,
[68]SCK-CEN, Nuclear Research Centre, 2400 Mol, Belgium,
[69]Second University of Napoli, Consorzio CREATE, Via Claudio 21, 80125 Napoli, Italy,
[70]Seoul National University, Shilim-Dong, Gwanak-Gu, Republic of Korea,
[71]Slovenian Fusion Association (SFA), Jozef Stefan Institute, Jamova 39, SI-1000 Ljubljana, Slovenia,
[72]Technical University of Denmark, Department of Physics, Bldg 309, DK-2800 Kgs Lyngby, Denmark,
[73]The "Horia Hulubei" National Institute for Physics and Nuclear Engineering, Magurele-Bucharest, Romania,
[74]The National Institute for Cryogenics and Isotopic Technology, Ramnicu Valcea, Romania,
[75]The National Institute for Laser, Plasma and Radiation Physics, Magurele-Bucharest, Romania,
[76]The National Institute for Optoelectronics, Magurele-Bucharest, Romania,
[77]Troitsk Insitute of Innovating and Thermonuclear Research (TRINITI), Troitsk 142190, Moscow Region, Russian Federation,
[78]Uni of Electronic Science & Tech of China, China,
[79]Unità Tecnica Fusione - ENEA C. R. Frascati - via E. Fermi 45, 00044 Frascati (Roma), Italy,
[80]Universidad Complutense de Madrid, Madrid, Spain,
[81]Universidad de Sevilla, Sevilla, Spain,
[82]Universidad Nacional de Educación a Distancia, Madrid, Spain,
[83]Universidad Politécnica de Madrid, Grupo I2A2, Madrid, Spain,
[84]Università di Roma Tor Vergata, Via del Politecnico 1, Roma, Italy,
[85]University College Cork (UCC), Ireland,
[86]University Milano-Bicocca, piazza della Scienza 3, 20126 Milano, Italy,
[87]University of Basilicata, Consorzio CREATE, Via Claudio 21, 80125 Napoli, Italy,
[88]University of California, 1111 Franklin St., Oakland, CA 94607, USA,
[89]University of Cassino, Consorzio CREATE, Via Claudio 21, 80125 Napoli, Italy,

[90]University of Helsinki, P.O. Box 43, FI-00014 University of Helsinki, Finland,
[91]University of Innsbruck, Fusion@Österreichische Akademie der Wissenschaften (ÖAW), Austria,
[92]University of Latvia, 19 Raina Blvd., Riga, LV 1586, Latvia,
[93]University of Lorraine, CNRS, UMR7198, YIJL, Nancy, France,
[94]University of Napoli "Federico II", Consorzio CREATE, Via Claudio 21, 80125 Napoli, Italy,
[95]University of Napoli Parthenope, Consorzio CREATE, Via Claudio 21, 80125 Napoli, Italy,
[96]University of Texas at Austin, Institute for Fusion Studies, Austin, TX 78712, Texas, USA,
[97]University of Tuscia,DEIM, Via del Paradiso 47, 01100 Viterbo, Italy,
[98]University of York, Heslington, York YO10 5DD, UK,
[99]Vienna University of Technology, Fusion@Österreichische Akademie der Wissenschaften (ÖAW), Austria,
[100]VTT Technical Research Centre of Finland, P.O.Box 1000, FIN-02044 VTT, Finland,
[101]Wigner Research Centre for Physics, P.O.B. 49, H - 1525 Budapest, Hungary,